Emulation Testbed for the Development of Lunar Surface Communication Systems

Matthew Hilts
NASA, 21000 Brookpark Rd. Cleveland, OH, 44135, matthew.hilts@nasa.gov
Tristin Pulsipher
NASA, 21000 Brookpark Rd. Cleveland, OH, 44135, tristin.pulsipher@nasa.gov
Lauryn Leslie
NASA, 21000 Brookpark Rd. Cleveland, OH, 44135, lauryn.leslie@nasa.gov
Michael Zemba
NASA, 21000 Brookpark Rd. Cleveland, OH, 44135, michael.zemba@nasa.gov
Aaron J Swank
NASA, 21000 Brookpark Rd. Cleveland, OH, 44135, a.j.swank@grc.nasa.gov

Abstract

As NASA's Artemis Program begins to establish a sustained human presence on the Moon, terrestrial surface-to-surface communication technologies will be used to connect many nodes across the lunar surface. Wi-Fi will be used for short range surface-to-surface links beginning on Artemis III. Third Generation Partnership Project (3GPP) technologies have been baselined for Artemis V, with a technology demonstration planned for Artemis III. Although these technologies are mature terrestrially, the lunar surface presents a more challenging and less-characterized radiofrequency (RF) environment. Thus, it is beneficial to perform evaluations of how 3GPP and Wi-Fi technologies will perform in advance of their deployment during Artemis. In this work, we present the Glenn Research Center (GRC) Emulation and Modeling (GEM) testbed: a hardware-in-the-loop emulation testbed designed for the prediction and evaluation of RF communication system performance on the lunar surface. GEM's architecture features ray-tracing-based channel models, a hardware RF channel emulator, and rapid reconfigurability of the 3GPP and Wi-Fi system components it uses to create the communication system under test. In this work, we present the architecture and initial laboratory build-up of GEM, with an emphasis on future expansion. To demonstrate GEM's functionality, we emulate two notional Artemis III extravehicular activity traverses. We show that the ray tracing simulation and subsequent 3GPP system performance in emulation show good agreement with expected lunar channel impairments.

1 Introduction

Within this decade, NASA's Artemis program will return to the Moon and begin establishing a sustained human presence on the lunar surface. Artemis will further our understanding of the Moon's geology and ice deposits, test methods of in-situ resource utilization, and demonstrate the critical technologies needed for future human missions to Mars [1]. A robust and scalable surface communications infrastructure is a necessity, both to enable a sustained presence on the Moon and to demonstrate the resilient architectures required for Mars [2]. This infrastructure will be required to connect many human and robotic network nodes on the lunar surface to each other and back to mission operation centers (MOCs) on Earth. Implementing individual lunar relay or direct-to-Earth (DTE) links for each node is inefficient and presents scalability issues, especially when connecting multiple nodes in close proximity on the lunar surface. Initial Artemis missions will employ Wi-Fi and NASA's legacy ultra-high frequency (UHF) space-to-space communication system (SSCS) to facilitate surface-to-surface communications. However, these technologies present challenges for surface operations. SSCS is primarily limited to voice transmissions and is not scalable to many users. While Wi-Fi is optimized for connecting many users, it is not well suited to long-range point-to-multipoint communications without modification. Both Wi-Fi and SSCS systems are unable to meet the maximum range requirements (10 km) for Lunar Terrain Vehicle (LTV) excursions [3].

In response to these challenges, NASA has adopted the use of terrestrial cellular communications standards to supplement Wi-Fi during Artemis. The specifications of the Third Generation Partnership Project (3GPP), such as 4G and 5G, will be demonstrated beginning with Artemis III and transition to operational capability for Artemis V. For an initial demonstration during Artemis III, Axiom Space, the prime contractor for the Artemis extravehicular activity (EVA) suits, has partnered with Nokia to demonstrate the performance of a 4G system for high-rate uplink during EVAs [4]. 3GPP technology promises to provide wide areas of coverage up to 10 km and efficient connectivity between surface nodes. Additionally, as lunar surface activity expands, 3GPP technology will enable network scalability and the aggregation of Earth-bound data to DTE trunk links.

Although 3GPP and Wi-Fi standards are mature in terrestrial applications, the lunar surface presents a more challenging and less-characterized radiofrequency (RF) propagation environment. Additionally, the unique nature of connecting lunar and terrestrial networks can introduce challenges for application layer software due to the lightspeed delay between the Earth and the Moon. To reduce risk and demonstrate these systems prior to launch, it is desirable to be able to predict and evaluate the performance of 3GPP and Wi-Fi systems in lunar-like RF environments. Such a capability could allow mission planners to quickly verify that astronauts will have reliable and high-rate (~10's Mbps) communications on their planned EVAs. Additionally, mission planners could select optimal landing sites or asset placement to maximize communications coverage in areas of interest. To meet this need, we present the Glenn Research Center (GRC) Emulation and Modeling (GEM) testbed: a hardware-in-the-loop emulation testbed designed for the prediction and evaluation of RF communication system performance on the lunar surface.

GEM is designed to be suitable for lunar surface communication system evaluation and analysis in the following ways. First, because mission planners need to verify communications performance over specific traverses, GEM utilizes ray tracing channel simulation software, rather than statistical models, to generate the channel models it uses in emulation. Second, GEM's architecture provides swappable options for testbed components, such as radio hardware and core network software. Automation allows changes between these components to be made rapidly, allowing the user to select whichever components best suit their testing needs. This is especially important in a less-characterized RF environment like the lunar surface, where switching between debugging, research-oriented components and performance testing components may be necessary in testing. Lastly, as Artemis progresses, commercial vendors may produce their own 3GPP and Wi-Fi components for use on the lunar surface. GEM is designed to incorporate these new devices as optional components for testing and evaluation under lunar channel conditions.

The paper is organized as follows. In section 2, GEM is compared to similar testbeds found in the literature. In section 3, GEM's architecture is described in detail and in section 4 the initial laboratory implementation is presented. Section 5 discusses the process GEM uses to generate and refine channel models for implementation in the hardware channel emulator. Finally, section 6 presents preliminary results from emulating two notional Artemis III 4G demonstration EVAs.

2 Related Work

3GPP and Wi-Fi emulation testbeds are abundant in the literature, each designed for a specific application. Examples of testbeds with similar designs to GEM include Colosseum [5], the 5G-SpaceLab testbed [6], and the urban vehicular test drive testbed at the University of Bristol (UoB) [7]. Colosseum is a large-scale "white-box" wireless testbed employing software defined radios (SDRs) and a Massive Channel Emulator (MCHEM) powered by CaST [8], a ray tracing toolchain for creating and characterizing realistic wireless network scenarios. 5G-SpaceLab deploys SDRs and a channel emulator with software tools including Ansys's Systems Tool Kit (STK) and Open Air Interface to emulate links from lunar surface assets to lunar orbital relays or DTE. The UoB testbed utilizes commercial off-the-shelf (COTS) user equipment (UE) hardware and the university's in-house ray tracing software to emulate user traverses across an urban environment.

GEM, while employing similar tools and methods, possesses a unique architecture driven by its use case. While Colosseum focuses on emulating a large volume of RF network nodes, which entails a maximum of four non-zero taps per tapped delay line (TDL) model due to computational limitations [8], GEM prioritizes high-fidelity channel emulation for less nodes, using up to 48 non-zero taps per TDL model. While the 5G-SpaceLab testbed focuses on the emulation of lunar relay and DTE links, especially the delay and Doppler effects, GEM prioritizes surface-to-surface link emulation, emphasizing multipath and diffraction effects. The UoB testbed utilizes a single set of UE and a single base station (BS) for system performance testing. In comparison, GEM is designed for rapid reconfiguration between research-oriented 3GPP components, COTS 3GPP components, and Wi-Fi components to support user testing needs.

In this effort we:

- Implement the first lunar-surface-focused 3GPP testbed with physical layer channel emulation.
- Outline a development path to include Wi-Fi components and refine the channel emulation.
- Evaluate the testbed's suitability for lunar surface RF emulation for the Artemis III 4G demonstration.
- Present emulation of two notional EVAs, showing that observed channel impairments are consistent with expectations of lunar surface propagation characteristics.

3 Architecture

GEM's emulation capabilities comprise both lunar surface and DTE links. While GEM emulates surface links at the RF layer, DTE links are emulated at the network layer using the Linux Network Emulator (NetEm) tool, which adds delay to link traffic to simulate the lightspeed delay between the Moon and the Earth. Although the DTE links are emulated at a higher layer and with less realism compared to the surface links, they allow GEM to evaluate application layer performance between lunar 3GPP networks and the Earth. RF layer DTE emulation is a planned future capability to address increased multipath at the lunar poles due the low elevation angle of Earth relative to the lunar horizon. The RF layer lunar surface link emulation and current network layer DTE link emulation are shown in Figure 1.

To emulate lunar surface links, GEM utilizes a Keysight Propsim F64 channel emulator and Ansys's STK and RF Channel Modeler (RFCM) software. Figure 1 shows the process GEM uses to generate channel models. Lunar mission scenarios are constructed in STK, utilizing digital elevation maps (DEMs) of the lunar surface. RFCM calculates the channel response between nodes in the STK simulation using

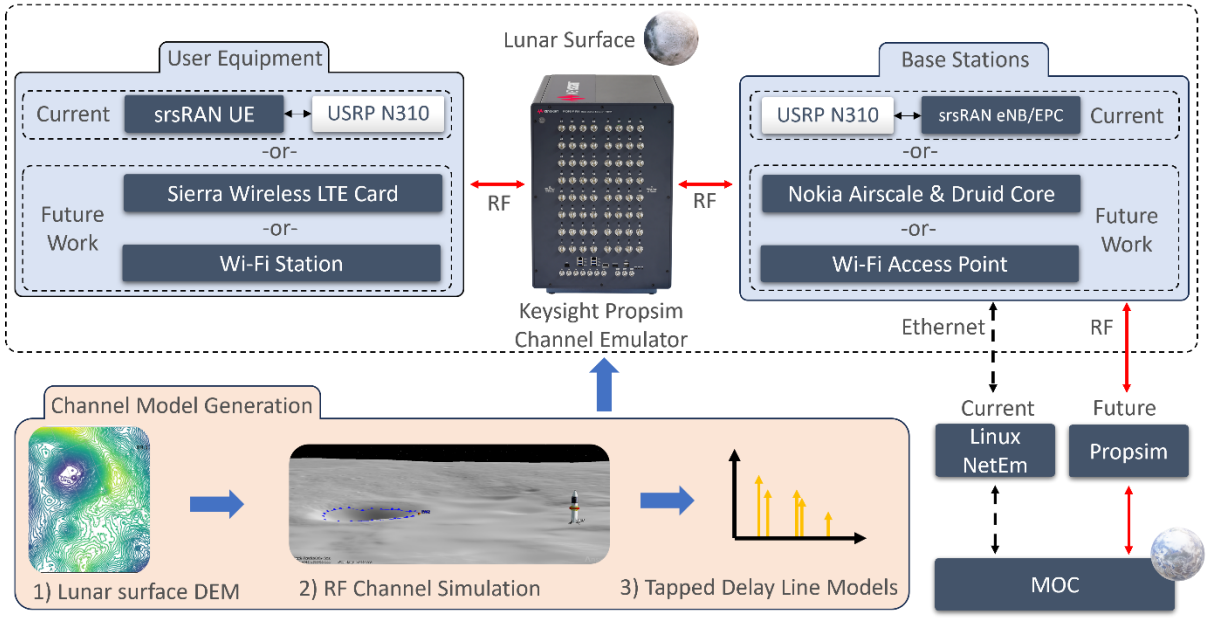

Figure 1: GEM architecture.

shooting and bouncing ray (SBR) techniques [9]. GEM software processes the channel response into a usable TDL model for the Propsim. The process of generating realistic channel models in RFCM and converting them for use in the Propsim is discussed in detail in section 5.

The ability to rapidly switch between different 3GPP and Wi-Fi components for each emulation is a key feature of GEM's architecture. This feature allows users to construct 3GPP and Wi-Fi systems with different characteristics to fit their testing needs. For example, a 3GPP system created with research-oriented hardware and open-source software allows a user transparency into the 3GPP stack and maximal ability to change system parameters. Because the lunar surface is less characterized than terrestrial environments, having complete access to the 3GPP stack and parameters may be important if unexpected system performance is observed in emulation. Future lunar 3GPP and Wi-Fi components are expected to be developed from chipsets with terrestrial heritage. Thus, a 3GPP or Wi-Fi system created using currently available COTS components will be more representative of systems that may be deployed on the Moon. However, COTS components tend to provide the user with less transparency. Figure 1 shows this concept, where the user has a choice of which components instantiate each UE and BS. Here, we use UE and BS as general terms and not in their 3GPP specific meanings. Multiple UEs and BSs can be instantiated in GEM to emulate networks of lunar surface links utilizing both 3GPP and Wi-Fi technology. Currently, GEM is configured to support up to two UEs and one BS, which will increase as GEM's development progresses.

In GEM's current stage of hardware development, UEs and BSs are realized using research-oriented hardware, specifically Ettus Universal Software Radio Peripherals (USRPs). A full 3GPP stack is run by the open-source RAN software srsRAN, on servers connected to each USRP [10]. Future work will include adding the option of COTS 3GPP components, specifically Sierra Wireless LTE transceiver cards, Nokia Airscale radios, and Druid Raemis 4G/5G Core network software, as well as COTS Wi-Fi components. As 3GPP and Wi-Fi components designed for deployment on the Moon are produced for Artemis, GEM will expand to incorporate flight spares or engineering models for performance testing before deployment.

Presently, there are no internationally accepted channel models for the lunar surface. The channel models that GEM uses, which are produced by STK and RFCM simulation, are currently validated by scarce amounts of empirical RF propagation data from the lunar surface. Future work will improve the realism of these channel models in the following ways. First, more validation data will become available from successful missions such as Commercial Lunar Payload Services (CLPS) landers, which will be used to refine simulation results. Second, channel soundings of lunar-analog locations on Earth will be collected, and compared to simulation results from those same locations. Third, Remcom's Wireless InSite channel simulation software will be used in tandem with RFCM. Agreement between two independent simulations will increase confidence in the accuracy of the resultant channel models. Additionally, each tool may be applied to specific use cases where it excels.

4 Hardware Implementation

GEM has been architected with extensibility and ease of use as core design principles. The current RF schematic for GEM is shown in Figure 2. Multiple RF switch matrices allow for rapid hardware configuration changes and future addition of COTS 3GPP and Wi-Fi components. A set of six couplers, labelled *spectrum analyzer couplers*, are utilized to tap the transmit and receive signals from each UE and BS to a selectable switch, which is connected to a spectrum analyzer. This allows each signal path to be viewed before and after the channel emulator and provides an insightful view on how the active channel model degrades the RF signal. Another set of four couplers, labelled *loopback couplers*, are used for loopback testing, minimizing the amount of RF switches required for connectivity troubleshooting.

Two major capabilities of GEM are its automation and reconfigurability. A custom-made web-based application named *GEM Commander* provides a GUI for interfacing with the testbed and can be operated on any machine on the laboratory network. It allows the operator to switch between spectrum analyzer views, turn loopback on or off, switch UE and BS hardware, start and stop the system under test, and control various network speed and streaming test applications. It is important to achieve simplicity of

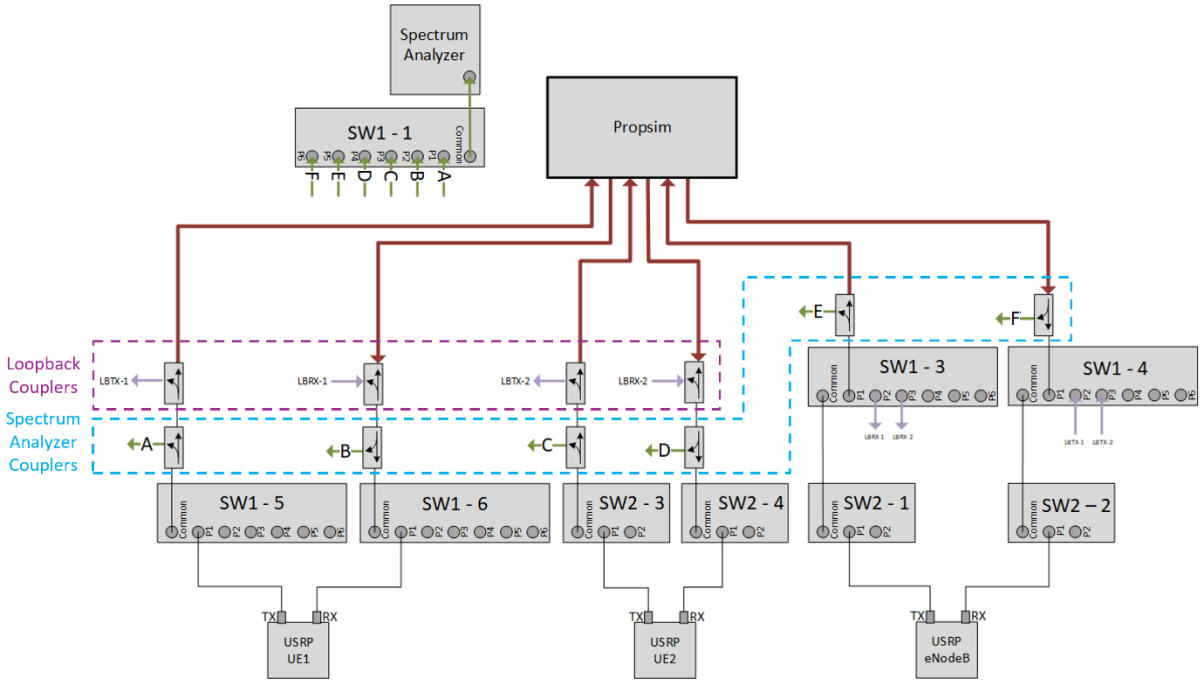

Figure 2: GEM RF schematic.

operation without completely abstracting the operator from the telemetry and configuration of the system under test. Thus, *GEM Commander* is designed to interface with each 3GPP and Wi-Fi component over the lab network and to forward system performance data to *GEM Commander's* host machine. Noticeable benefits of *GEM Commander* have been significantly reduced system setup time, minimized operator error, repeatable test conditions, and fast training of new testbed operators.

The current rack configuration of GEM is shown in Figure 3. Each instance of srsRAN is hosted on an independent Dell PowerEdge R450 sever, which has 16 GB of RAM and is running Ubuntu Linux. These servers are each connected to a USRP N310 via a 10 Gb SFP fiber connection. In future work, Nokia Airscale radios will be added to the testbed along with Druid Raemis 4G/5G Core network software. These commercial products will act as an alternative 3GPP BS that can be switched in or out of the testbed via

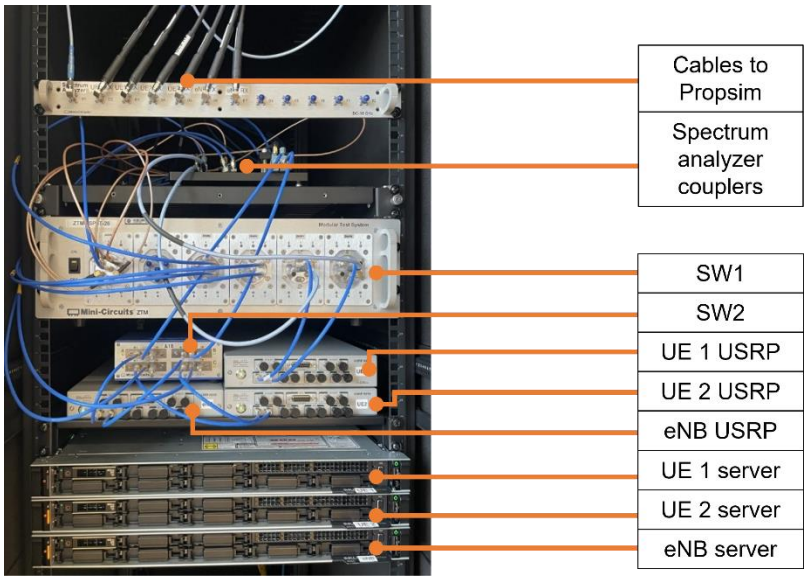

Figure 3: GEM rack setup.

GEM Commander. Single board computers (SBCs) with Sierra Wireless LTE transceiver cards will expand 3GPP UE device options. SBCs will also be used as Wi-Fi UE devices by removing their built-in Wi-Fi antenna, converting to a wired coaxial connection, and connecting into GEM's RF switch matrix. A commercial Wi-Fi access point with coaxial connections will be added as a Wi-Fi BS device.

5 Channel Modeling

GEM utilizes Ansys's STK and RFCM software to generate channel models, which the Propsim uses for channel emulation. RFCM is a software package that brings SBR channel sounding into STK's scenario analysis. The ability to generate channel models within simulated EVA scenarios (STK + RFCM) is a key feature that makes GEM useful for mission planners. This section is organized as follows: section 5.1 discusses the process of using STK and RFCM to generate channel models and section 5.2 discusses the processing needed to convert these models into usable files for the Propsim.

5.1 Channel Simulation

To begin modeling a scenario, a DEM of the lunar surface area of interest is converted into a 3D terrain tileset via an STK utility. Next, the tileset is loaded into STK and combined with any scene contributing objects, such as landing vehicles, deployed equipment, or fine terrain features not captured in the DEM (boulders or rocks smaller than the DEM resolution, typically on the order of 1 – 5 m). Within RFCM, transmitters, receivers, and antenna patterns are added to the desired objects in the scenario and lunar regolith RF parameters are assigned to the 3D tileset (relative permittivity $\epsilon_r = 3.4$, conductivity $\sigma = 0.005$ S/m [11]). Additionally, the RFCM parameters shown in Table 1 are set to the user's preference.

Table 1: Example RFCM Parameters

RFCM Parameter	Variable	Example Value	
RF Channel Frequency (GHz)	f_c	2.5	
Channel Bandwidth (MHz)	BW	200	
Frequency Samples / Sounding	N_{freq}	1024	
Sounding Interval (msec)	T_{sound}	1000	
Sounding / Analysis Time Step	N_{sound}	1	
Unambiguous Channel Delay (µsec)	τ_{max}	5.12	(read only)
Unambiguous Channel Distance (m)	R_{max}	1534.937	(read only)

During simulation, RFCM generates one channel frequency response (CFR) per channel sounding. Each CFR is calculated by performing an SBR simulation and results in N_{freq} frequency samples spaced evenly across the bandwidth, BW. CFRs are generated periodically during the simulation, with a frequency of $1/T_{sound}$. This results in N_{CFRs} CFRs, each N_{freq} samples long, where N_{CFRs} can be calculated by dividing the total simulation time by T_{sound}. Taking the inverse Fourier transform of each CFR yields the band-limited channel impulse response (CIR), hereafter referred to simply as the CIR. The simulation bandwidth, BW, defines the time domain resolution, Δt, of the CIR, calculated by (1).

$$\Delta t = \frac{1}{BW} \tag{1}$$

The unambiguous channel delay, τ_{max}, which is a measure of how long the delay spread of the channel can be before aliasing will occur, is calculated by (2).

$$\tau_{max} = \frac{N_{freq}}{BW} \tag{2}$$

The unambiguous channel distance, R_{max}, which is a measure of how far reflections can travel before aliasing will occur, is calculated by (3), where c is the speed of light.

$$R_{max} = \frac{N_{freq}}{BW} * c \quad (3)$$

Thus, when setting values for bandwidth and number of samples per sounding, the user needs to ensure that the unambiguous channel distance is greater than the maximum distance to an expected reflector in the scenario.

While work to generate more detailed channel models is ongoing, the following RFCM configuration choices yield good agreement with expected channel characteristics. First, the UE node is set to be the SBR transmitter, and the BS node is set to be the SBR receiver. This configuration is preferred for both uplink and downlink analyses such that the ray-shoot emanates from the mobile user. The antenna on the UE node follows the current position of the mobile user and is closer to the ground than the antenna on the BS node. Therefore, the UE antenna is generally in closer proximity to relevant terrain features than the BS antenna and the ray density is highest near terrain features of interest (such as crater rims). Similarly, setting the ray density parameter of the SBR simulation to a value greater than 1 ray per wavelength has yielded better results than the default value of 0.1, which is likely due to GEM's analysis over longer distances (500 m – 10 km). These longer distances necessitate higher than standard ray density to increase interactions with distant terrain features. Lastly, the simulation bandwidth is set to 200 MHz. This choice is determined by the channel emulator and CIR trimming process that GEM utilizes and is discussed in greater detail in section 5.2.

5.2 Emulation Pre-Processing

Hardware TDL channel emulators are generally more resource limited than software channel simulators. These constraints include the dynamic range of the taps, the minimum spacing between the taps, and the number of non-zero taps a channel emulator can realize per CIR. These limitations constitute one major reason the pre-processing of channel simulation data is needed before it can be used in channel emulators. For our Propsim model, these limits are about 100 dB of dynamic range, a 5 ns tap spacing grid and 48 taps per CIR. RFCM simulation data is prepared for use in the Propsim via Algorithm 1, as follows.

Algorithm 1

Inputs:

$\boldsymbol{CFRs}_{N_{CFRs}\,x\,N_{freq}}$ (RFCM CFRs matrix, N_{CFRs} by N_{freq})

Outputs:

$\boldsymbol{Coeffs}_{N_{CFRs}x\,48}$ (TDL coefficients matrix, N_{CFRs} by 48)

$\boldsymbol{Delays}_{N_{CFRs}x\,48}$ (TDL delays matrix, N_{CFRs} by 48)

$\boldsymbol{N}_{N_{CFRs}\,x\,1}$ (CIR normalization factors matrix)

$G_{baseline}$ (Baseline gain through the Propsim)

Start:

for i $\in \{1, \dots, N_{CFRs}\}$ **do** (For each CFR index)

$CIR \leftarrow IFT\{\boldsymbol{CFR}_i\}$ (Take the IFT of the CFR)

$CIR_{delays} \leftarrow$ top 48 indices of $|CIR|$ (Add top 48 indices by magnitude to delays)

$CIR_{trimmed} \leftarrow CIR[CIR_{delays}]$ (Add values for top 48 indices to trimmed)

$CIR_{delays} \leftarrow CIR_{delays} * \Delta t$ (Turn delay indices into seconds)

$CIR_{peak\,tap} \leftarrow \max(|CIR_{trimmed}|)$ (Find max magnitude sample in trimmed CIR)

$CIR_{trimmed} \leftarrow \frac{CIR_{trimmed}}{CIR_{peak\,tap}}$ (Normalize the trimmed CIR)

$\boldsymbol{Coeffs_i} \leftarrow CIR_{trimmed}$ (Add trimmed samples to **coeffs** row)

$\boldsymbol{Delays_i} \leftarrow CIR_{delays}$ (Add delays to **delays** row)

$\boldsymbol{N_i} \leftarrow |CIR_{peak\,tap}|$ (Add CIR peak tap mag to normalization set)

$G_{baseline} \leftarrow \max(N)$ (Define the baseline gain)

$N \leftarrow \frac{N}{G_{baseline}}$ (Normalize the normalization matrix)

For each CFR in the RFCM simulation output, Algorithm 1 converts the CFR to a CIR via the inverse Fourier transform and then trims the CIR down to the top 48 samples by magnitude. To most effectively utilize the Propsim's dynamic range, each trimmed CIR is normalized such that the sample with maximum magnitude is set to 0 dB. The normalization factors used for each CIR are recorded sequentially in a matrix, $\boldsymbol{N}$, which is then itself normalized such that the maximum normalization factor is 0 dB. The value used to normalize $\boldsymbol{N}$ is referred to as the baseline gain, $G_{baseline}$.

To load the output of Algorithm 1 into the Propsim, the following steps are performed. First, the trimmed and normalized CIR samples in the $\boldsymbol{Coeffs}$ matrix and the corresponding delay values in the $\boldsymbol{Delays}$ matrix are loaded into the Propsim's channel editor as the TDL model. Next, the normalization matrix is loaded into the channel editor as the "shadowing profile", which defines variable attenuation over scenario time. Finally, the output gain of the Propsim is adjusted such that the combination of output gain, baseline channel model loss and cable losses to and from the Propsim equals $G_{baseline}$.

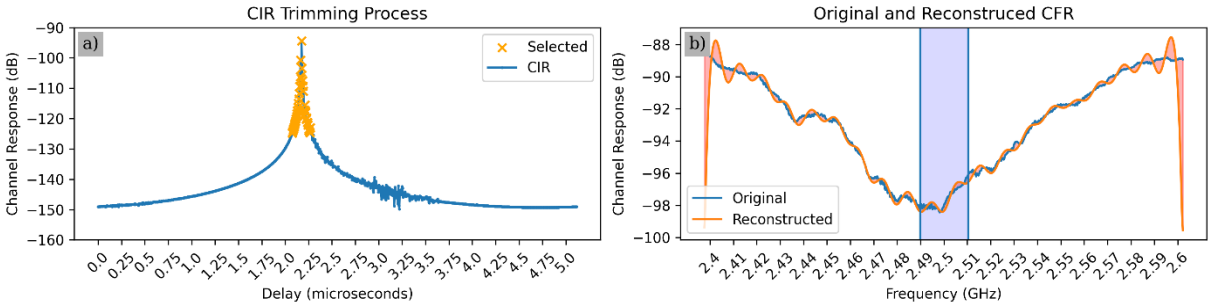

Figure 4: a) Algorithm 1's trimming process and b) comparison of the original and reconstructed channel frequency response.

An example of Algorithm 1's CIR trimming process is shown in Figure 4a, where the CIR is trimmed to the 48 taps with the largest magnitude. Figure 4b shows a comparison between RFCM's output CFR and the reconstructed CFR produced by taking the Fourier transform of the trimmed CIR. In general, the trimmed CIR produces a CFR in good agreement with the original. The largest error occurs at the edges of the emulation bandwidth where the effects of Gibb's phenomenon can be seen. Thus, the emulation error for a signal is minimal if the signal's bandwidth is small compared to the emulation bandwidth, and the signal is at the emulation's center frequency. This is shown in Figure 4b, where the blue shaded region shows the center 20 MHz of the emulation bandwidth. In this example, the average percent error between the original and reconstructed CFRs in the full 200 MHz band is 2.29%, while the average percent error in the middle 20 MHz is 1.43%. The worst percent error for an individual frequency sample in the full 200 MHz band is 111.67% and the worst percent error in the middle 20 MHz is 5.79%. For 4G systems which are usually limited to a maximum bandwidth of 20 MHz, Algorithm 1, combined with the 5 ns tap spacing of the Propsim, allows for low emulation error across the signal bandwidth. However, for 5G systems that can exceed 200 MHz of bandwidth, the emulation error from Algorithm 1 will be more significant.

The trimming method employed in Algorithm 1 is extremely simple and is designed to maximize the accuracy of the CFR reconstruction in emulation. Several studies have proposed other methods of preparing ray-tracing-based channel simulation data for use in resource constrained channel emulators [12, 13, 14]. These methods emphasize accuracy in one or more of the following areas: CFR, power delay profile, mean delay, RMS delay spread and path loss [12]. In future work, algorithms that provide optimal emulation accuracy in the CFR, delay spread, and path loss will be investigated and integrated into GEM.

6 Preliminary Testing Results

To demonstrate the operation of GEM, two notional Artemis III 4G demonstration EVAs are emulated. During the demonstration, each astronaut on EVA will communicate with the Human Landing System (HLS) via a 3GPP UE. The HLS will host an evolved Node B (eNB) and an evolved packet core (EPC). For GEM's demonstration, a notional HLS landing site (86.9064 °S, 20.2603 °W) in the Haworth crater

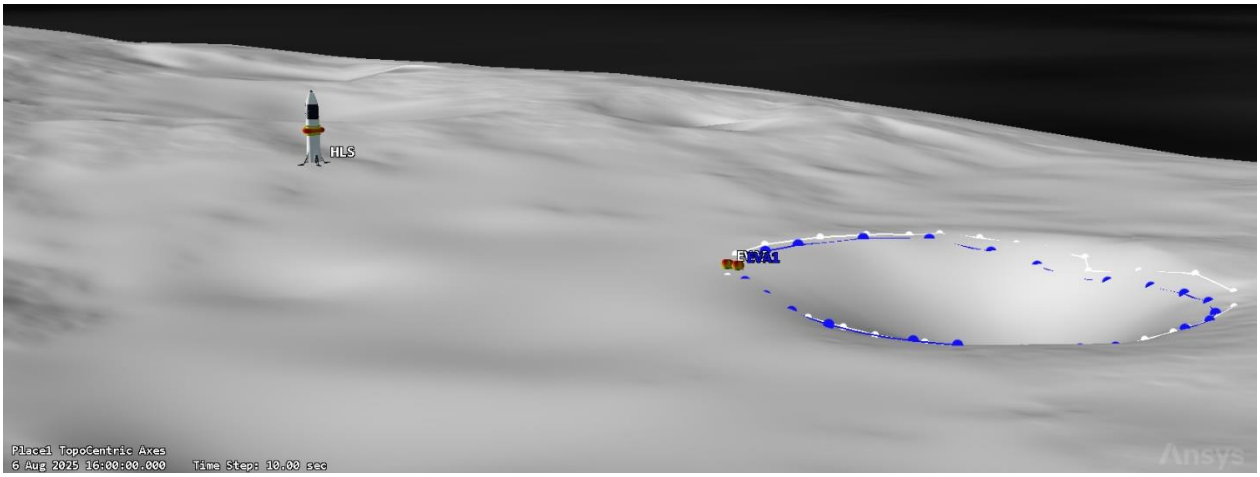

Figure 5: STK Simulation of two notional Artemis III 4G demonstration EVAs.

area near the lunar south pole is selected. This site is 619 meters away from a crater, which has a radius of 139 meters.

A 3D tileset of the Haworth crater area is generated from a 1-meter resolution photoclinometry DEM [15], and imported into STK. Then, STK nodes representing the HLS and both EVAs are added in. The EVAs are set to circle the crater in a counterclockwise manner moving 0.5 meters per second, which takes a total of 28.5 minutes (1711 seconds) to complete. Within RFCM, notional antenna patterns for each UE and the eNB are imported. The UE antennas are set to be 2 meters above the surface, and the eNB antenna, assumed to be mounted on the HLS, is set to 30 meters above the surface. The STK scenario is shown in Figure 5.

Four separate channel sounding simulations are performed, one for each EVA's uplink (2560 MHz) and downlink (2860 MHz) frequency. For each channel sounding, 1711 CFRs are obtained, one for each second of the simulation. Figure 6 shows the CFR set for EVA 2's uplink channel (6a), compared with the reconstructed CFR set after Algorithm 1's CIR trimming method is applied (6b). The mean error between each frequency sample in 6a, and the corresponding frequency sample in 6b, is 4.03%. The percent error

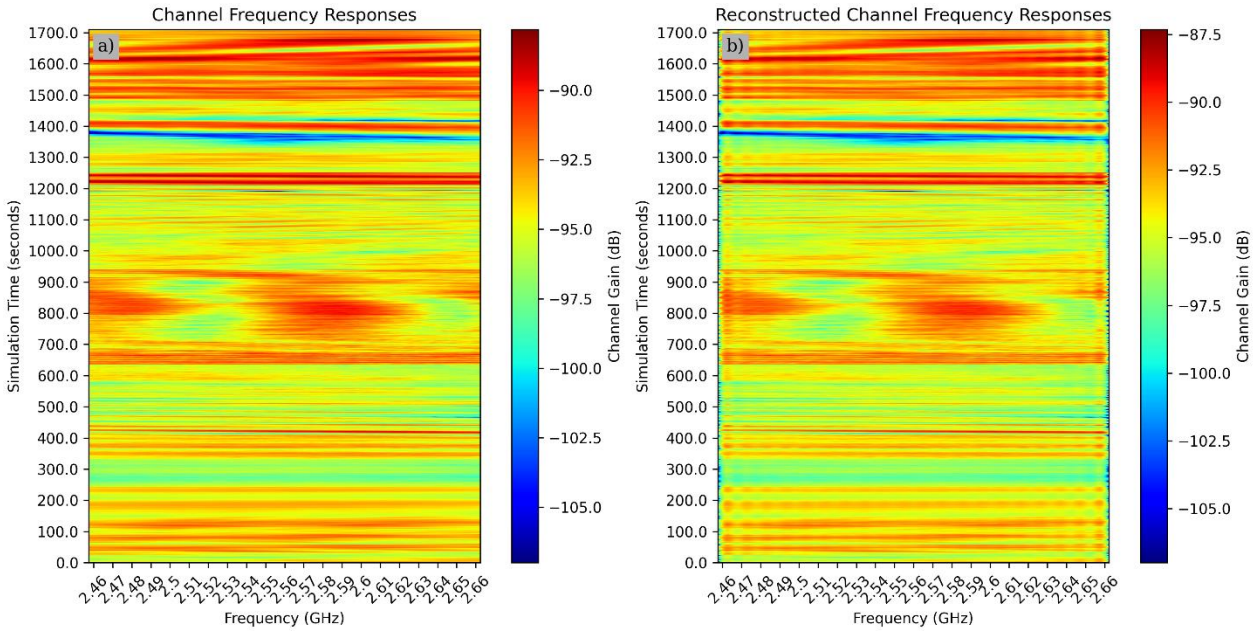

Figure 6: a) Channel Frequency Response vs Time and b) Reconstructed Channel Frequency Response vs Time.

two standard deviations above the mean is 8.49%. Within the central 20 MHz of each CFR, the mean error is 1.76% and the percent error two standard deviations above the mean is 3.65%. Future work will include updating Algorithm 1 to enforce a percent error that is under a certain set threshold.

Preliminary conclusions can be drawn about the agreement of the RFCM channel simulation data with expected channel characteristics. Between 250 and 350 seconds, the EVAs pass out of line of sight of the HLS, resulting in a period of shadowing. Figure 6 shows the simulation capturing this, where the overall signal power decreases evenly across the band during the shadowing period. Additionally, Figure 6 shows frequency selective fading occurring in the middle of the simulation, from about 700 to 1100 seconds. This shows good agreement with the expectation that multipath reflections will occur in an environment with extreme topology, like a crater. Figure 7 shows two selections of EVA 2's reconstructed CFRs that showed interesting channel characteristics: from 900 seconds to 1000 seconds (7a) and 1300 seconds to 1400 seconds (7b). The blue boxes denote the 20 MHz band through which a 4G signal is transmitted during emulation. Figure 7a shows frequency selective fading across the full band, and to a lesser extent, across the central 20 MHz. Figure 7b shows a deep fade in the central 20 MHz, created by a strong reflection in the environment.

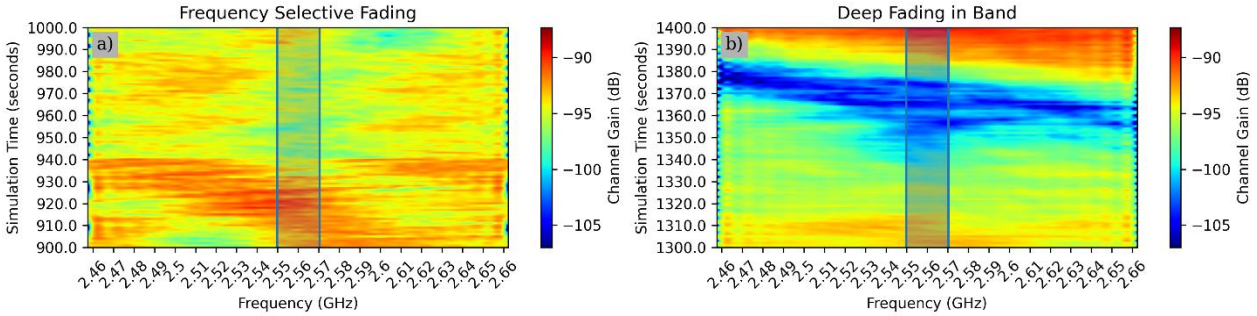

Figure 7: Zoomed in sections of the Channel Frequency Responses, a) 900 to 1000 seconds and b) 1300 to 1400 seconds.

Figure 8a shows EVA 2's CIRs, which are computed by taking the inverse Fourier transform of the CFRs. When astronauts are in view of the HLS (everywhere except 250 to 350 seconds), the highest power sample in each CIR represents the line-of-sight signal path. Each CIR bin is 5 ns apart and corresponds to 1.498 meters of lightspeed distance. Because the distance between the EVAs and the HLS is not always an integer multiple of 1.498 meters, leakage will occur. This phenomenon shows up as the bands of high energy which spread across both sides of the line of sight. Figure 8b shows the CIRs obtained by windowing each CFR with a Blackman window before taking the inverse Fourier transform, which is done to reduce the effects of leakage and make the multipath reflections easier to see. Figure 8b shows good agreement with the expectation that multipath reflections will occur when a crater is part of the environmental topology.

Next, the emulation is prepared. To realize the 3GPP system under test, GEM utilizes USRP N310s connected to servers running srsRAN. The USRPs are connected via GEM's RF switch matrix to the Propsim, which internally connects each UE USRP to the eNB USRP. The trimmed and normalized CIRs and the normalization matrix $\boldsymbol{N}$ are loaded into the Propsim for each of the four simulated channels. In the Artemis III 4G demonstration, the UEs will be Power Class 3, entailing a maximum output power of 23 dBm. Because USRP N310s cannot transmit at that power, 23 dB is added to $G_{baseline}$, and the USRPs are set to transmit at 0 dBm. Then the output gain in the Propsim is set such that total loss through the Propsim equals the $G_{baseline}$.

To begin the emulation, the EPC, eNB, and UEs are all turned on, and the Propsim plays through each CIR in sequence, one per second. While the channel is running, uplink data is generated using iperf, and the bitrate, signal to noise ratio (SNR), block error rate (BLER) and modulation and coding scheme (MCS) are all recorded. We focus on the uplink metrics because most of the data traveling between the

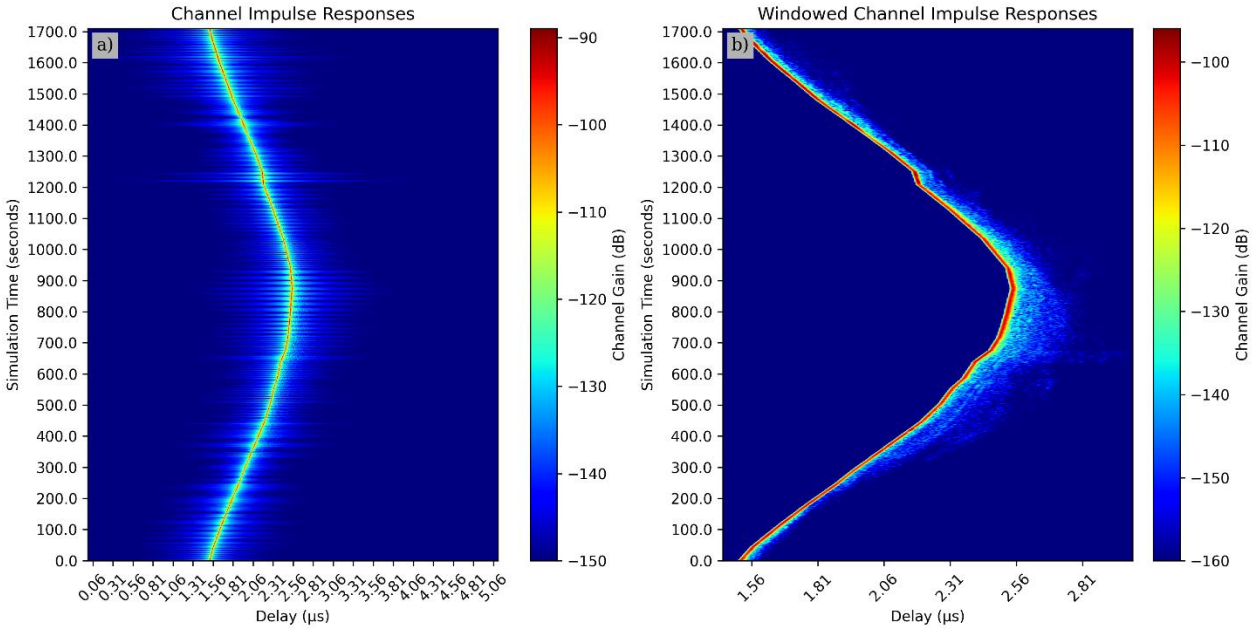

Figure 8: a) Channel Impulse Response vs Time and b) Windowed Channel Impulse Response vs Time.

astronauts and the HLS will be in the uplink, especially high-definition video streams. Figure 9 shows these metrics recorded for EVAs 1 and 2 during the emulation.

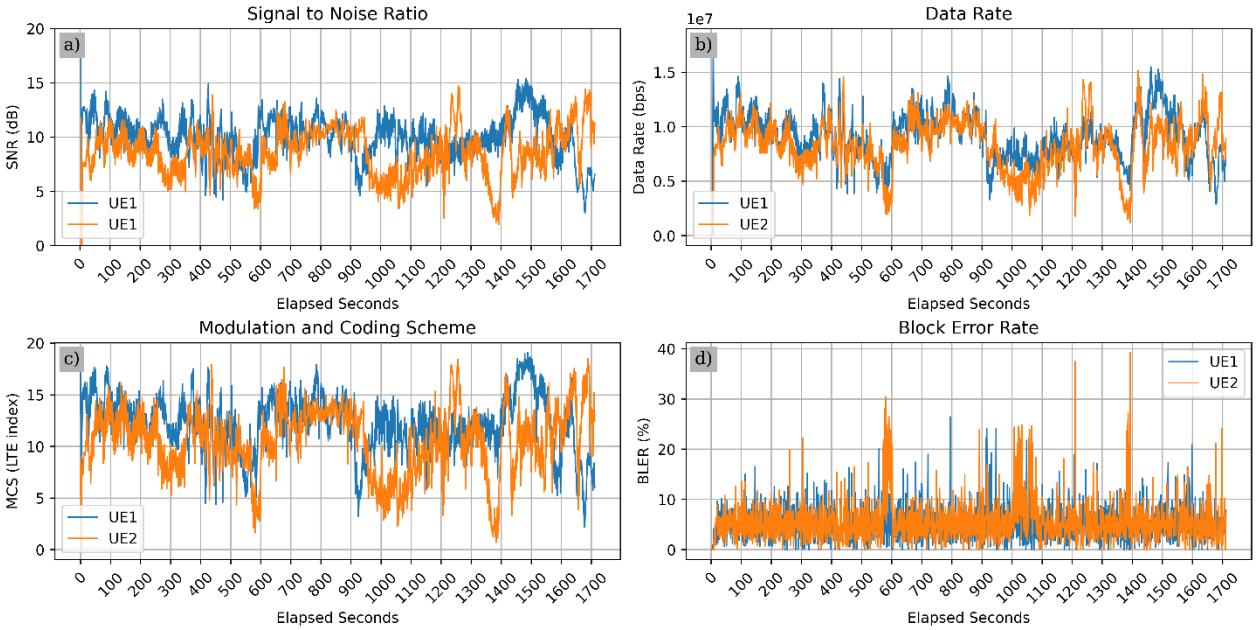

Figure 9: a) Signal to Noise Ratio, b) data rate, c) modulation and coding scheme and d) block error rate.

Due to the current lack of empirical measurements of 3GPP system performance on the lunar surface, direct comparison of the emulation results to reality is not possible. However, the emulation results align reasonably well with expected system behavior. For example, during the period from 250 to 350 seconds where the EVAs experience shadowing (see Figure 6), the SNR drops, which results in a lower MCS and data rate, as well as a few spikes in BLER. During the periods of 950 to 1100 seconds and 1350 to 1400 seconds, EVA 2 encounters high channel fading. During these periods, EVA 2 experiences drops in SNR and spikes in BLER, which correspond to lower MCS values and data throughput. Future work will improve system metric processing and analysis, as well as investigate system dynamics such as failure

recovery speed and traffic flow in combined 3GPP/Wi-Fi networks. In this work it suffices to show that initial emulation test results demonstrate good agreement with expected system behavior.

6. Conclusion

In this paper, we present GEM: a hardware-in-the-loop emulation testbed designed for the prediction and evaluation of RF communication system performance on the lunar surface. GEM is designed to allow mission planners to emulate channel conditions for EVAs on the Lunar surface and to evaluate the performance of 3GPP and Wi-Fi systems in those channel environments. Rapid reconfigurability of 3GPP and Wi-Fi system components is a key feature of GEM, allowing users the ability to select components suitable for their testing needs. Currently, GEM uses USRPs and srsRAN to realize 3GPP system components. Future work will add in COTS 3GPP and Wi-Fi components as options. We present a simple channel simulation processing algorithm that provides reasonable (<10% average error) emulated CFR reconstruction for the scenario we emulate in this paper. In future work, channel simulation realism will increase and more optimal channel simulation to emulation processing algorithms will be utilized. We demonstrate the operational readiness of GEM through the emulation of two notional Artemis III 4G demonstration EVAs and show that the initial results of these emulations show good agreement with expected channel characteristics and system performance.

Acknowledgements

This work was funded by the National Aeronautics and Space Administration (NASA) Space Communications and Navigation (SCaN) program in the Space Operations Mission Directorate and was performed under the Lunar 3GPP project at the NASA Glenn Research Center. The Lunar 3GPP project is jointly led with the Johnson Space Center (JSC) Exploration Wireless Lab (JEWL) and the authors would like to thank Dr. Raymond Wagner, Chatwin Lansdowne, and William Dell for their support throughout GEM's development. The project is also grateful to early advocates for the use of 3GPP technology on the lunar surface across NASA and industry, including Bernie Edwards of the NASA's Space Technology Mission Directorate (STMD) and too many others to enumerate here. The authors would also like to acknowledge commercial partners Ansys, Keysight, and Remcom for their thorough support in the novel application of their channel modeling tools to unique lunar use cases. Lastly, the authors would also like to thank cooperative partners in academia who have supported Lunar 3GPP, GEM, and JEWL, including but not limited to: Oscar Somerlock, Julia Andrusenko, and Brian Choi of Johns Hopkins University Applied Physics Laboratory; Dr. Stephen Braham of Simon Fraser University; and Dr. Kevin Gifford of the University of Colorado Boulder.

References

[1] S. Creech et al, "Artemis: An Overview of NASA's Activities to Return Humans to the Moon", IEEE Aerospace Conference, Big Sky, United States, March 2022

[2] "Moon to Mars Objectives", National Aeronautics and Space Administration, September 2022

[3] B. Edwards et al, "3GPP Mobile Telecommunications Technology on the Moon", 2023 IEEE Aerospace Conference, Big Sky, MT, USA, 2023, pp. 1-12

[4] K. Coggins et al, "NASA's Approach to Lunar Communication and Navigation: Artemis and Beyond", 75th International Astronautical Congress (IAC), Milan, Italy, October 2024.

[5] L. Bonati et al, "Colosseum: Large-Scale Wireless Experimentation Through Hardware-in-the-Loop Network Emulation", 2021 IEEE International Symposium on Dynamic Spectrum Access Networks (DySPAN), Los Angeles, CA, USA, 2021, pp. 105-113

[6] O. Kodheli et al, "5G Space Communications Lab: Reaching New Heights", 18th International Conference on Distributed Computing in Sensor Systems (DCOSS), Marina del Rey, Los Angeles, CA, USA, 2022, pp. 349-356

[7] M. Charitos et al, "LTE-A Virtual Drive Testing for Vehicular Environments", 2017 IEEE 85th Vehicular Technology Conference (VTC Spring), Sydney, NSW, Australia, 2017, pp. 1-5

[8] D. Villa et al, "CaST: a toolchain for creating and characterizing realistic wireless network emulation scenarios", in *Proc. 16th ACM Workshop on Wireless Network Testbeds, Experimental Evaluation & Characterization (ACM MobiCom '22)*, Oct. 2022, pp. 45–52.

[9] Ansys, “RF Channel Modeler: High-Fidelity Wireless Channel Modeling in Dynamic Virtual Terrestrial Environments”, January 2024
[10] Software Radio Systems, “srsRAN 4G Documentation”, Release 23.11, February 2025
[11] M. Karam et al, “Electrical Properties of Lunar Environment Used for Predicting Lunar RF Propagation Characteristics”, May 2024
[12] A. W. Mbugua et al, "On Simplification of Ray Tracing Channels in Radio Channel Emulators for Device Testing", 2021 15th European Conference on Antennas and Propagation (EuCAP), Dusseldorf, Germany, 2021, pp. 1-5
[13] C. Mehlfuhrer et al, "Approximation and resampling of tapped delay line channel models with guaranteed channel properties", 2008 IEEE International Conference on Acoustics, Speech and Signal Processing, Las Vegas, NV, USA, 2008, pp. 2869-2872
[14] A. W. Mbugua et al, "Efficient Preprocessing of Site-Specific Radio Channels for Virtual Drive Testing in Hardware Emulators", in IEEE Transactions on Aerospace and Electronic Systems, April 2023, vol. 59, no. 2, pp. 1787-1799
[15] M. O’Connor et al, “Lunar LRO NAC Haworth Photoclinometry DEM 1m”, https://astrogeology.usgs.gov/search/map/lunar_lro_nac_haworth_photoclinometry_dem_1m (accessed August 8, 2025)